Modeling the Dynamics of Salt Marsh Development in Coastal Land Reclamation

Yiyang Xu[1], Tarandeep S. Kalra[2], Neil K. Ganju[3], Sergio Fagherazzi[1]

[1]Department of Earth and Environment, Boston University, Boston MA 02215, USA

[2]Aperture Inc., Contractor to the U.S. Geological Survey, Herndon, VA 20171, USA

[3]U.S, Geological Survey, Woods Hole, MA 02543, USA

Key words: marsh restoration, land reclamation, COAWST, vegetation dynamics, phases of marsh development, expectance of marsh coverage

Key Points

1. Marsh formation can be divided in three distinctive phases: preparation phase, encroachment phase, and adjustment phase.
2. Sediment concentration, settling velocity, sea level rise, and tidal range each comparably affect restoration outcomes in different ways.
3. Our simulations show that the Unvegetated-Vegetated Ratio (UVVR) also relates to sediment budget in marsh development.

Abstract

The valuable ecosystem services of salt marshes are spurring marsh restoration projects around the world. However, it is difficult to determine the final vegetated area based on physical drivers. Herein, we use a 3D fully coupled vegetation-hydrodynamic-morphological modeling system to simulate the final vegetation cover and the timescale to reach it under various forcing conditions. Marsh development in our simulations can be divided in three distinctive phases: a preparation phase characterized by sediment accumulation in the absence of vegetation, an encroachment phase in which the vegetated area grows, and an adjustment phase in which the vegetated area remains relatively constant while marsh accretes vertically to compensate for sea level rise. Sediment concentration, settling velocity, sea level rise, and tidal range each comparably affect equilibrium coverage and timescale in different ways. Our simulations show that the Unvegetated-Vegetated Ratio also relates to sediment budget in marsh development under most conditions.

Plain language summary

The valuable ecosystem services of salt marshes are spurring marsh restoration projects around the world. Given their important role in shore protection and carbon sequestration, marsh restoration and expansion projects are becoming more common. However, it is difficult to

predict the final extension of the vegetated area in a restored marsh and what drivers control vegetation cover. In this study, a state of the art numerical model was used to simulate marsh development in a typical configuration used in land reclamation projects. The final vegetation cover and the timescale to reach it are derived from simulations with various sediment conditions, tides, and sea level rise. We found that marsh development can be divided in three distinctive phases: a preparation phase characterized by sediment accumulation in the absence of vegetation, an encroachment phase in which the vegetated area grows, and an adjustment phase in which the vegetated area remains relatively constant while marsh platforms rise vertically to compensate for sea level rise. Sediment concentration, settling velocity, sea level rise and tidal ranges each plays a role in terms of equilibrium coverage and the time needed to reach it.

1. Introduction

Salt marshes are valuable and unique landforms located at the interface between land and ocean. Salt marshes are still common along many shorelines, despite a 25% decline of the original coverage and a current 1~2% rate of loss per year (Crooks et al., 2011; Duarte et al., 2008; "Secretariat of the Convention on Biological Diversity," 2007). The most recent estimate of global marsh area exceeds 5 million Ha (Mcowen et al., 2017). Serving as a natural defense, salt marshes play an important role in reducing the damage of storms to coastal communities (Möller et al., 2014; Temmerman et al., 2013; Zhao & Chen, 2014). In the United States, shoreline protection by marshes against storms are valued up to $5 million per km^2 (Costanza et al., 2008), and coastal wetlands were valued at $625 million in protecting against direct flood damages during Hurricane Sandy (Narayan et al., 2017). Other valuable ecosystem services provided by salt marshes include nutrient removal, carbon storage, and habitat for flora and fauna (Zedler & Kercher, 2005). Therefore, salt marshes not only protect coastal communities but also sustain economies and

55 healthy ecosystems. Recognizing the above services, multiple public and private agencies are
56 attempting to create and sustain marshes (Barbier et al., 2008; Bayraktarov et al., 2016; Seddon et
57 al., 2020). Restoration practices include shoreline protection, sediment trapping, and thin layer
58 sediment placement techniques among others (VanZomeren et al., 2018; Wigand et al., 2017).
59 These techniques are implemented in existing marsh systems to prevent marsh degradation or
60 promote marsh expansion. Other projects aim at creating new marsh land using engineered
61 structures

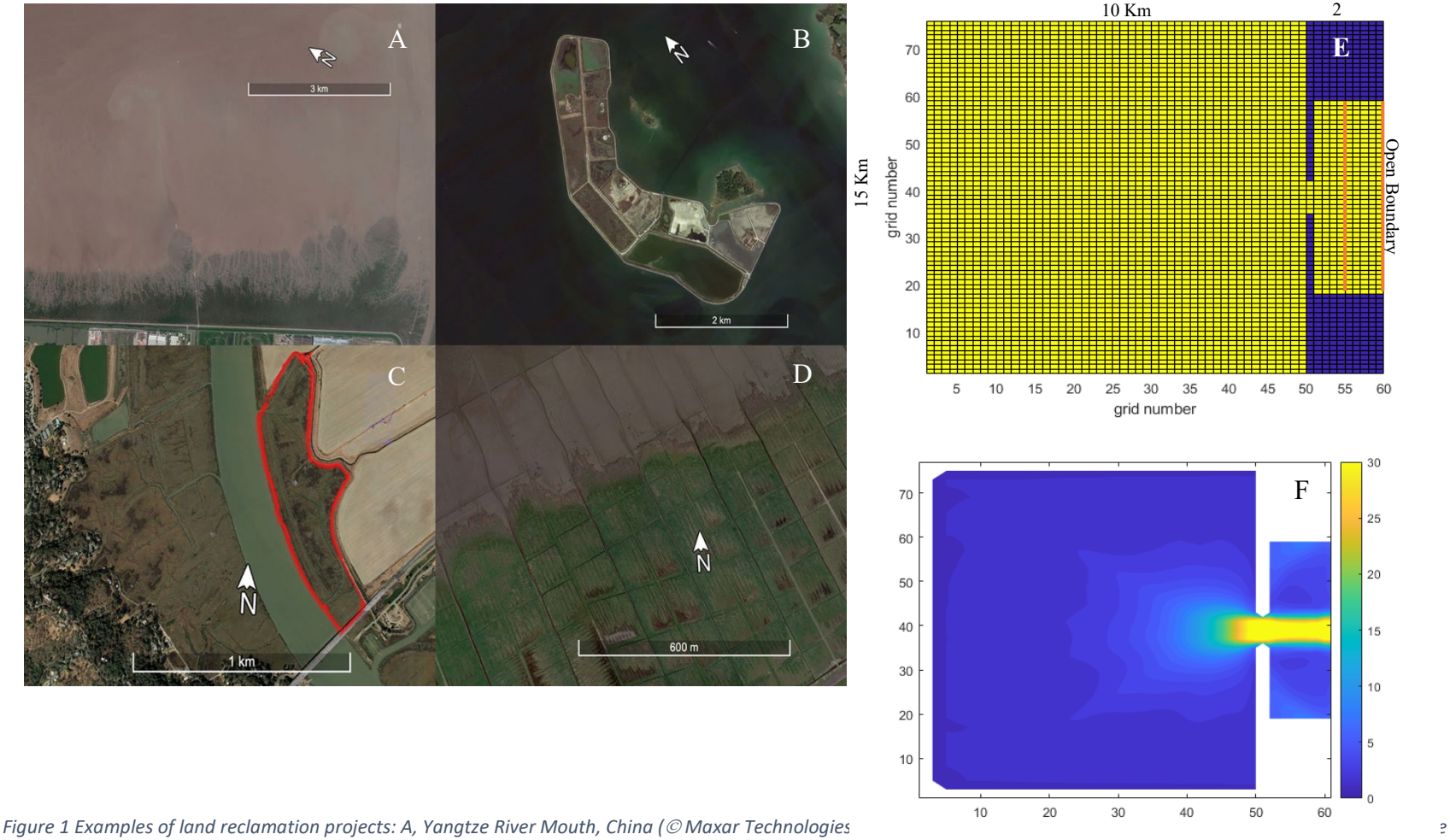

Figure 1 Examples of land reclamation projects: A, Yangtze River Mouth, China (© Maxar Technologies Bay, USA (Data SIO, NOAA, U.S. Navy, NGA, GEBCO, © TerrainMetrics 2021 © Google 2021). C, Petaluma River Marsh Restoration, USA (© Google 2021). D, coastal expansion near Groninger Wad, The Netherlands (© GeoBasis-DE/BKG 2021 © Google 2021). E, Model geometry. Cells in yellow are active during simulation, the two orange line signify where hydrodynamic and sedimentary open boundary conditions were imposed. F, bathymetry after tidal spin ups. Bathymetry for each different tidal range settings were separately created by a 30 days run where only hydrodynamics affect the bed this is a tidal spin up to adjust bathymetry to the hydrodynamics.

63 (Staver et al., 2020); while some studies show that engineered marshes do not always lead to
64 sediment gains (Fleri et al., 2019), some others indicate that restoration blocks sediment export
65 while protecting the marsh from wave erosion (Vona et al., 2020). Thus different outcomes can
66 emerge from restoration projects.
67 A common configuration of these engineered marsh projects are sea walls or dikes shaping a
68 rectangular area with an inlet to the ocean or estuary (Fig. 1). This geometry mimics natural inlet
69 systems, which creates asymmetric tidal velocities leading to net sediment transport from the ocean
70 into bays (Brown & Davies, 2010; Pingree & Griffiths, 1979). The net sediment transport across
71 an inlet depends on the morphology and marsh vegetation in the back barrier basin (Elias et al.,
72 2012; Mariotti & Canestrelli, 2017).
73 Assessing the likelihood of marsh survival in response to SLR (Sea Level Rise) has been
74 the focus of research for several decades Click or tap here to enter text.(Fagherazzi et al., 2012;
75 Mckee & Patrick, 1988; Morris & Haskin, 1990). Sediment supply has been identified as a key
76 factor to determine marsh survival (Mariotti & Fagherazzi, 2010) as well as success in marsh
77 restoration (Ganju, 2019). Under different SLR scenarios, reaching marsh equilibrium requires
78 different sediment supply (Fagherazzi et al., 2013). The ratio between unvegetated and vegetated
79 area (Unvegetated Vegetated Ratio, UVVR) in a marsh system has been proposed as a simple
80 metric to assess sediment budgets and resilience against SLR (Ganju et al., 2017). UVVR scales
81 well with sediment budget that indicates healthy (sediment import) or unhealthy (sediment export)
82 marshes, and it is easily measurable through satellite images. However, more work is needed to
83 understand the relationship of UVVR with other parameters that lead to marsh development. The
84 present work attempts to close this data gap. We simulate marsh development under a wide range

of scenarios and unravel the link between vegetated marsh surfaces and different forcing conditions.

The driving forces of marsh development vary from site to site, so controlled long-term studies are needed that test sediment conditions, tidal range, and SLR. Computer models have the advantage of comparability and flexibility in studying marsh dynamics. Multiple models have been developed and applied to study salt marsh landscapes. Many efforts have been made to couple marsh vegetation and sedimentation processes (Nardin et al., 2016; Nardin & Edmonds, 2014; Temmerman et al., 2005) as well as morphology and vegetation (D'Alpaos et al., 2007; Kirwan & Murray, n.d.; Mariotti & Fagherazzi, 2010; Morris, 2006; Mudd et al., 2004). Mariotti and Canestrelli (2017) studied an idealized tidal basin with a fully coupled model but applied limited testing to external forcing (sediment concentration and SLR). Other models that simulated mangroves or marshes have focused on the channel network (Marciano et al., 2005; van Maanen et al., 2015). Alizad et al., (2016) developed a model for studying salt marsh development in tidal estuaries and applied it to Timucuan salt marsh system (northeast Florida). The model calculated biomass density based on marsh elevation and tidal datum that led to a geospatial accretion in marsh domain. The elevation change of marsh platform led to a modified bottom friction and altered tidal dynamics. However, the model did not consider dynamic sediment transport.

In this work, we use a coupled vegetation-hydrodynamic-morphological model to study the development of a marsh via vegetation colonization and its relationship with forcing conditions. The Coupled-Ocean-Atmosphere-Wave-Sediment Transport (COAWST) Modeling System (Warner et al., 2010) is used, with a newly developed vegetation module (Kalra et al., 2021). We were able to simulate marsh development in an idealized basin and monitor sediment fluxes and feedbacks with vegetation through a varying range of sediment, SLR, and tidal conditions. This is

the first modeling study aimed at predicting the final equilibrium marsh coverage in response to various forcing conditions. Our results are important for marsh restoration and land reclamation as we provide the final vegetation coverage and the timescale to reach it for a range of forcing variables.

2. Methods

First, we introduce the numerical model with a description of the newly developed method to simulate marsh development. Then, we detail the model domain set-up and modules used for the simulations. Finally, we present the modifications that we implemented on the hydrodynamic and vegetation components of the model.

2.1 Model description for marsh development

The modeling framework (COAWST v3.7) has various components responsible for coastal processes including but not limited to hydrodynamics, sediment transport, vegetation, and terrain evolution. Details on model coupling can be found in Warner et al (2010). For the application presented in this work, we adopted the sediment transport and marsh routines presented in Kalra et al. (2021). Updated model framework can be found in supplemental materials (Fig. S5)

The long-term formation of the marsh is modeled by accelerating the process of deposition and erosion with a morphological factor of 200 (Ranasinghe et al., 2011; Roelvink, 2006; Warner et al., 2010). The deposition or erosion caused by the hydrodynamics are multiplied by this factor and then added to or subtracted from the bed. However, this multiplication only happens at the interface of water and bed sediment, therefore, the sediment concentration in the water column is not affected by it. We initialize the model with sufficient bed sediment (10 meters of sediment layer) to allow for erosion as we are using a large morphological factor.

2.2 Design of numerical experiments

We design an idealized case that mimics a natural inlet basin in a barrier island system or an engineering structure built for land reclamation that naturally imports sediment (Fig. 1A~D). We then adopt realistic values of sea level rise, tidal range, sediment concentration, and grain size (Table 2 in supplement) and force them at the open boundary (Fig. 1E). Tides were varied in amplitude only, with uniform period of 12 hours for all simulations so we can relate outcomes to the effect of tidal range. In each case, only one kind of sediment was simulated. Since we focus on the colonization and evolution of intertidal marshes in sheltered areas, we do not consider waves for simplicity.

The domain consists of square grid cells (dx = 200 m in the horizontal) with 10 Sigma layers. The open boundary is 8 km wide and 15 m deep, while the inlet is 1.2 km wide (Fig. 1E). The basin area is 145 km^2 with a uniform water depth of 2 m and with an additional random elevation of ± 0.05 m. Density and porosity of the bed sediment were fixed across experiments while grain size changes with settling velocity in different simulations (Table 2 in supplement). The four cases of settling velocity (STL0.1~STL0.5) each only simulates a single sediment grain-size. Across scenarios, we simulated five grain sizes including the standard case.

We also specify an area about 1 km wide near the open boundary where sediment deposition is not allowed (Fig. 1E). This area mimics the surf zone where the flow conditions are strong enough to maintain sediment in suspension without deposition. Specifically, all settling fluxes of sediment through vertical layers were set to zero so that grid elements in contact with this area inherit the sediment concentration at the boundary. By doing this, we allow the hydrodynamics to develop according to our geometric configuration while sediment concentrations remained as they were prescribed at the boundary. Settling fluxes were then linearly

increased to model-calculated values between the end of this area and the inlet. This configuration allows us to constrain the sediment input and net budget to the system.

2.3 Simulations

The vegetation routine was modified to represent the development of a tidal marsh and to optimize model performance (Fig. S5). The model was initiated with a bare flat basin. During the simulation, a cell is converted to a marsh cell only when it reaches a threshold elevation and gets dry at low tide for the first time. Then following the parabolic distribution (equation 1 in supplement), the biomass is updated based on elevation and hydroperiod parameters in each time step. In Table S1 (supplement), we report a list of parameters used in the simulations. A spin-up run was conducted for each tidal range case (Table S2, Fig. 1F). The goal of the spin-up run is to reach an equilibrium depth at the inlet so the filling of the basin occurs as a result of sediment import from the ocean. To simulate SLR, we keep the mean water level unchanged and uniformly decrease the bottom elevation of the entire domain.

2.4 Optimal UVVR and timescale analysis

Vegetation coverage is calculated with the Unvegetated-Vegetated ratio (UVVR) first proposed by Ganju et al., (2017). In order to determine the equilibrium UVVR and the time it takes to reach it, we regress the UVVR-time series with equation 1.

$$UVVR = E(1 + Ae^{-bt}) \quad (1)$$

E represents the asymptotic value that UVVR will eventually reach. The percentage of total area covered by marshes is therefore $\frac{1}{1+E}$. A reflects the curvature of the fitted curve and b controls the velocity at which the equilibrium is reached. t_{95} is defined as time (t) needed to reach 95% of the equilibrium vegetated area. This method works for most cases as long as the system reaches

equilibrium. In case of very high SLR (exceeding 25 mm/year), a stable marsh area cannot establish, and thus these are not included as we are providing an expectation to stable formation of marsh.

3. Results

First, we examine the evolution of a specific simulation which serves as a standard case (Std). Then, results from each set of experiments where one of the four independent variables (SLR rates, sediment input, settling velocity, or tidal range) is varied are presented.

3.1 Standard Case

The Std case adopts SLR, sedimentary conditions, and tidal range (Table 1 in supplement) from observations near the artificial land-gaining structure at the Yangtze River mouth (Ai et al., 2018). By analyzing the time series of marsh biomass and UVVR, we find that UVVR reaches a stable value much earlier than marsh biomass (Fig. 2 & Fig. S4). In the Std case (Table S2), UVVR variations decrease to less than 1/1000 of its variance after 25 years, while marsh biomass variations are minimal after 40 years (Fig. S4).

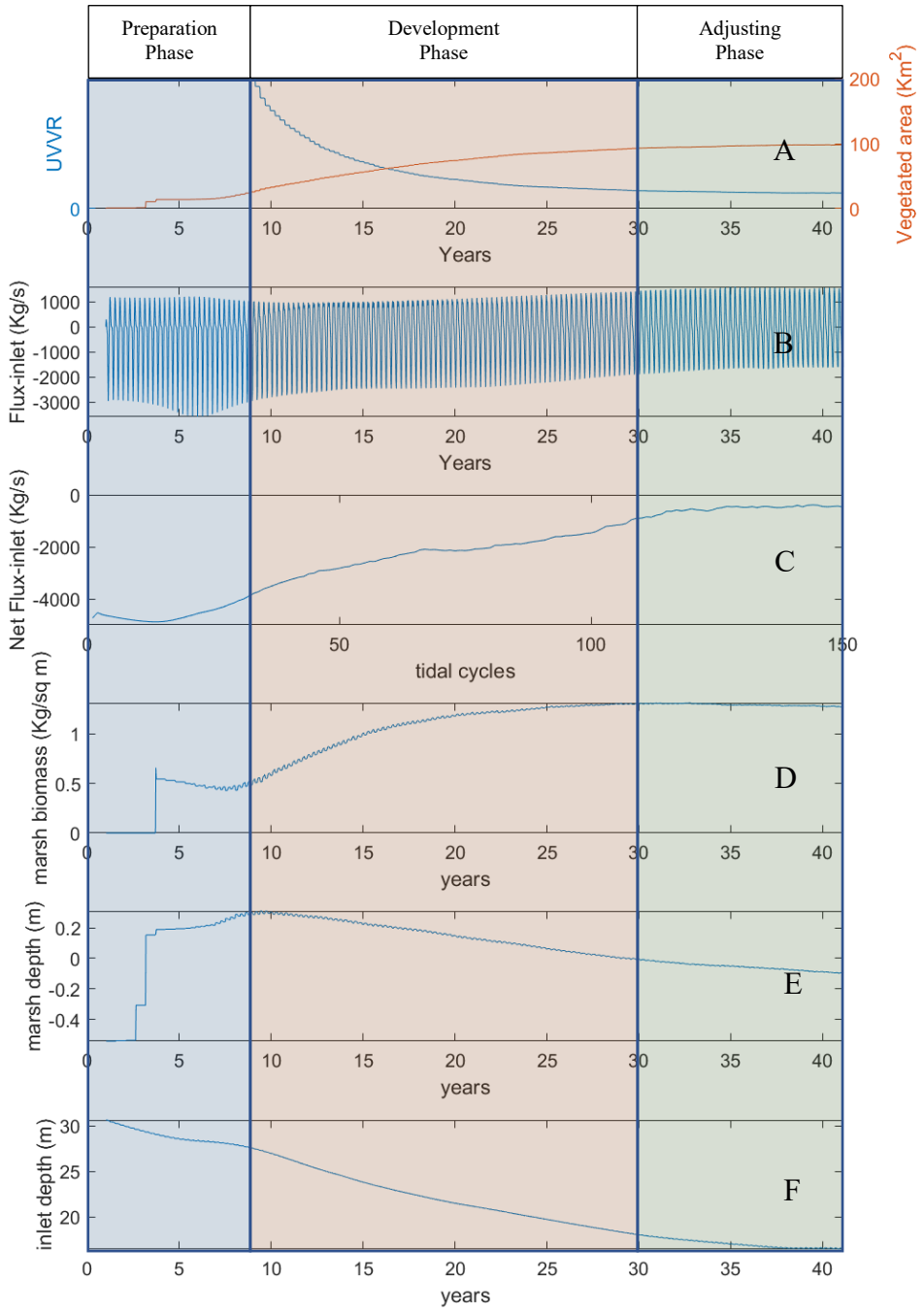

Figure 2. Development of marsh over time. Color zones indicate phases of marsh development. a) UVVR, b) sediment flux (Kg/s) at the inlet, c) net sediment flux at the inlet (Kg/s) for each tidal cycle, d) average marsh biomass (Kg/m²), e) average water depth (m) on the marsh platform, e) average water depth(m) at the inlet. The simulation is with SLR=5mm/yr.

189

190 At the beginning of the simulation, there is a period of rapid import of sand for around 35 tidal
191 cycles, which is equivalent to about 9 years (area shaded in blue in Fig. 2). The net import of
192 sediment through the inlet was on average 4516 kg/s. Most sediment enters the bay while a small
193 fraction fills the inlet as shown in Fig. 2F as well as in Fig. S2A&B. At the end of the preparation
194 phase, the inlet is slowly filling, the bay is accreting and vegetation starts to colonize the basin
195 (Fig. S2B). The slow filling of the inlet (0.73 m/year of average inlet bathymetric change) is due
196 to a reduction in tidal prism, which decreases the flow at the inlet, triggering deposition. The
197 sediment imported in this period fills the bay and brings the bottom elevation close to the threshold
198 for vegetation colonization. The UVVR value was high during the first 10 years, meaning there
199 was little or no land in the suitable elevation range for vegetation. As we can see in Fig. S2-B, at
200 the end of this period the bottom of the bay is characterized by different depositional areas with
201 channels dissecting them and supplying sediment from the inlet. The bottom slope in the deep-
202 water area close to the inlet remains similar to the starting bathymetry, while the flat areas near the
203 boundaries are silting up. We name this period "Preparation Phase" as it serves the purpose of
204 preparing suitable areas for marsh colonization. It ends with a significant increase in marsh
205 biomass per unit area.
206 The next phase, called herein "Encroachment Phase" and shaded in green in Fig. 2, lasts
207 about 20 years, and it is characterized by salt marsh colonization. Percent of vegetation coverage
208 increases from 22% to 59%. Sediment import continues but with a decreasing rate (2193 Kg/s on
209 average). Through time, the flux of sediment favors an expansion of the salt marshes and promotes
210 accretion in the area already colonized by vegetation (Fig. 2A&E). In this period, the unvegetated
211 area near the inlet becomes shallower. As the rate of sediment import drops, the speed of marsh

212 expansion decreases (from 1008 m^2/day to 183.6 m^2/day). Fig. S2-C shows the end bathymetry of
213 this period, when the entire bay is filled with the exception of the large channels near the inlet.

214 The system eventually reaches equilibrium in terms of planimetric marsh area, with
215 dendritic channels dissecting the marsh and an area of deep water around the inlet. In the last phase,
216 named Adjustment Phase (shaded green area in Fig. 2), the marsh area remains relatively
217 unchanged while the marsh elevation is increasing to keep pace with SLR. In this phase the marsh
218 is accreting to compensate SLR. The marsh coverage represented by UVVR in Fig. 2A remains
219 stable for the last 5~10 years while the platform elevation keeps pace with SLR (Fig. 2D&E).

220 ### 3.2 Response to SLR, Tidal Range, and Sediment Characteristics

221 Equation 1 fits well the data with R^2 = 0.998 for the Std case. Generally, a lower equilibrium
222 UVVR is accompanied by a lower timescale to reach equilibrium. When conditions favor a large
223 marsh area, usually vegetation can reach that coverage faster (Fig. 3A).

224 The equilibrium UVVR is very high for low input sediment concentration (0.005 kg/m^3) and
225 decreases for higher concentrations. The decrease is more noticeable between 0.05 and 0.1 kg/m^3,
226 suggesting that there might be a minimum sediment supply required to facilitate vegetation
227 colonization (Fig. 3A). A larger settling velocity means more sediment can deposit in suitable
228 locations for vegetation colonization during high tide. Therefore, with a high settling velocity, the
229 equilibrium UVVR decreases and it is accompanied by a small equilibrium time (Fig. 3B). If the
230 sediment settles even faster than what we simulated here, a limit on the transport might present in
231 our domain. SLR hinders marsh expansion so equilibrium is reached with a smaller coverage and
232 with a time delay. However, at low rates of SLR, the time needed to reach equilibrium remains
233 constant, while at high rates it increases significantly. Despite t_{95} increasing nonlinearly with SLR,
234 the equilibrium UVVR grows linearly (Fig. 3C).

235

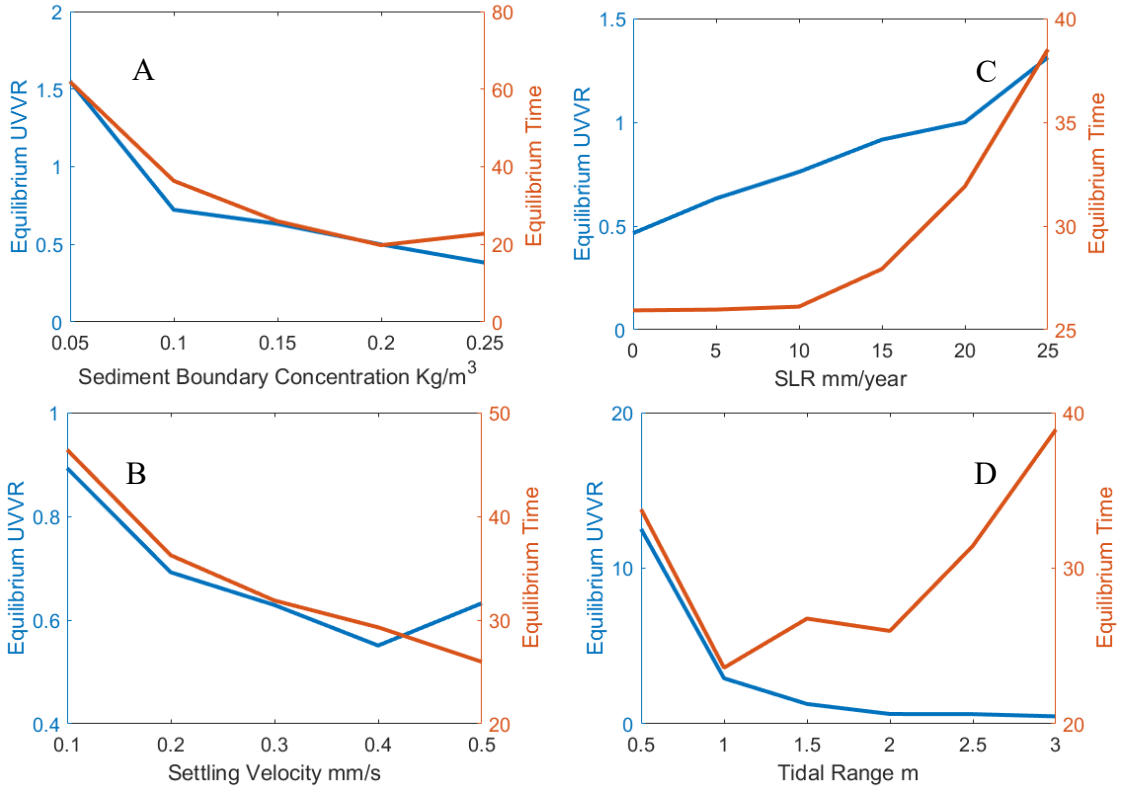

Figure 3 Equilibrium UVVR and time it takes to reach 95% of the equilibrium UVVR (equilibrium time) as a function of A: Sediment concentration as input at the boundary (kg/m³), B: Settling velocity of sand (mm/s), C: SLR (mm/year), D: Tidal Range (m).

The effect of tidal range is complex. The equilibrium marsh coverage increases when tidal range increases, while the t_{95} indicates that there is an optimal interval of tidal ranges for vegetation development (Fig. 3D). A tidal range too small or too large slows down marsh expansion. In microtidal environments the tidal prism is small, and this leads to limited fluxes of sediment toward the marsh.

4. Discussion

Previous studies have shown dependence of marsh development on various external factors such as sediment availability (DeLaune et al., 1990), land subsidence, or change of tidal water levels (Cole, 1994). Our results show that within the tested conditions, marsh restoration or land reclamation projects had optimal spatiotemporal coverage. With a 3D model, we found that short-term equilibrium was achieved by a rapid initial import of sand and vegetation encroachment: when the vegetated area is established, marsh accretion follows. This short-term equilibrium where marshes are able to maintain a constant extent is informative for guiding coastal marsh restoration and land reclamation.

As mentioned in the previous section, we expect marsh evolution to go through three phases, and a small tidal range will make the "Preparation phase" especially challenging as it requires a large amount of sediment flux to prepare the bay for vegetation. Thus, a high vegetation area could only be reached when the tidal range produces adequate sediment fluxes to go through the "Preparation phase" and perhaps "Encroachment phase" fast. On the other hand, a large tidal range not only brings more sediment; it also enlarges the tidal flow and thus bottom shear stress within a tidal cycle leaving a deposition much harder (Fagherazzi & Priestas, 2010 Fig. 4).. This leads to a delay in reaching equilibrium, since large amount of sediment flow in and out of the basin but little actually deposits.

Marshes tend to maintain smaller area when forced with higher SLR rates. Similar results were found by Mariotti and Canestrelli (2017) on marsh resilience to SLR, but our results were somewhat different when describing equilibrium marsh area. First, all SLR rates are constant in this study, meaning the sediment needed for the existing marshes to keep up with sea level rise does not change over time. A higher SLR will create more space to be filled in by the same amount of sediment input if other conditions remain the same. So the only way to keep up with SLR and maintain a stable marsh area is to focus deposition on a limited area and use the given sediment to build up vertically.

Marsh systems respond to SLR through sediment fluxes (Ganju et al. 2017). Degrading marshes showed evidence of co-evolving UVVR and sediment budget i.e., the more negative the sediment budget, the higher is UVVR. Also, SLR amplified net sediment export in an engineered tidal marsh site (Fleri et al., 2019). Ganju et al. (2017) only studied degrading marshes, but here we focus on a forming marsh and determine the relationship between UVVR and sediment fluxes.

In a forming marsh, sediment surplus decreases in time from high initial values to a value around 0.05 kg m^{-2} $year^{-1}$, while UVVR is also decreasing due to vegetation encroachment (Fig. 4a). The four time steps (10, 20, 30 and 40 years) in each set of experiments represent a variety of systems at different stages of marsh development (Fig. 4). Systems that evolved closer to equilibrium maintain a lower sediment budget because the system is in the "Adjustment phase." These systems generally keep up with SLR, and the net sediment import goes to vertical accretion of the marshes. On the other end of the spectrum, systems that are just starting vegetation colonization import sediment at a significantly higher rate than older ones. Overall, the sediment budget scales well with UVVR in most cases. Combining our results with Ganju et al (2017), a higher UVVR leads to greater sediment flux with importing fluxes in forming marshes and exporting in degrading

marshes. A lower UVVR is often accompanied by small sediment fluxes and reflects a near equilibrium state.

285

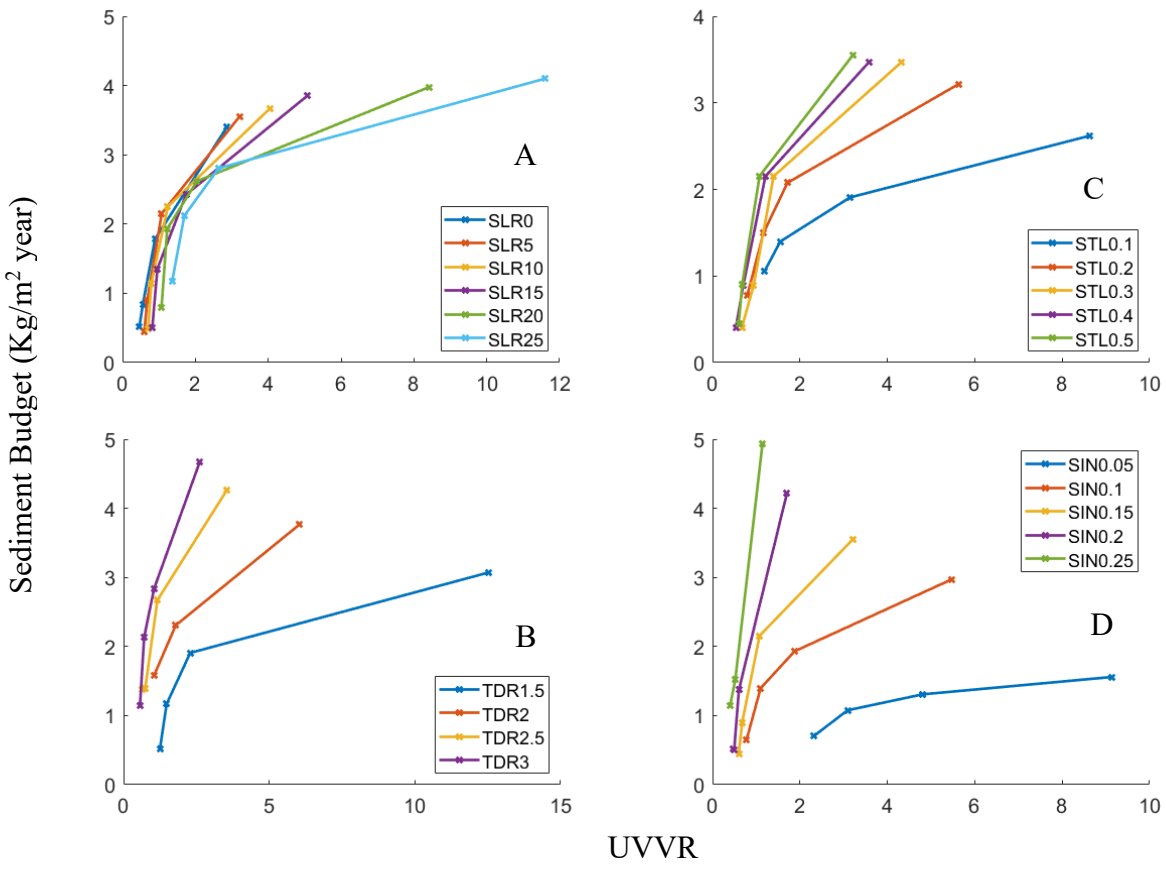

Figure 4 Sediment budget vs UVVR during salt marsh development with different forcing; each trajectory was simplified in four time steps: 10, 20, 30 and 40 years since the reclamation project started. A, SLR rates 0~25 mm/year. B,Tidal ranges 1.5~3 meters. C, settling velocities 0.1~0.5 mm/s. D, sediment inputs 0.05~0.25 kg/m^3.

Most models of marsh evolution are vertically integrated and tend to exaggerate bottom friction. This problem could be significant as vegetation produces vertically variant momentum extraction as well as turbulence across the water column (Beudin et al., 2017; Marjoribanks et al., 2014; Sheng et al., 2012). In our 3D hydrodynamics, velocity tends to be higher near the surface and lower at the bottom while sediment concentration appeared the opposite. Crucial parameters like sediment flux, deposition, or erosion are often products of multiplying velocity derived variables (bottom stress, turbulence, or flow speed itself) and sediment concentration. Not resolving vertical variance leads to potential overestimates of these parameters. Models that couple morphology and biology either simulate a transect over a long period of time or use a simplification of the hydrodynamics to determine the two-dimensional structure of a salt marsh, typically focusing on the channel network. The study carried out by Mariotti and Canestrelli (2017) only investigated two variables: sediment input and SLR, while not addressing the important effect of tidal range and settling velocity of different sediments.

5. Conclusion

Marsh restoration projects have been carried out for decades with little comprehensive understanding of what controls the final vegetation coverage and the time needed to reach that coverage. Our results close this gap by providing the final vegetation cover (UVVR) and the timescale to reach equilibrium under a variety of forcing conditions. SLR inhibits marsh expansion, thus leading to a lower final vegetation coverage and a longer equilibrium time to obtain that coverage. SLR rates higher than 25 mm/year might behave differently than what has been shown here and can be addressed in future studies. Restoration projects with more sediment supply and fine sediments are more likely to succeed in a short timeframe. The equilibrium marsh coverage

increases with tidal range but only moderate tides (1~2 meters) favor fast colonization. UVVR related well with sediment budget in forming marshes. High UVVR coincides with rapid sediment import, while low UVVR indicates marshes approaching equilibrium that need limited amount of sediment to keep up with SLR. We also identified three phases of marsh development : a Preparation Phase characterized by abiotic deposition, an Encroachment Phase in which vegetation colonizes the intertidal area, and an Adjustment Phase where the vegetated area is constant and accretion balances SLR.

These results can help predict future restoration outcomes and provide important data for coastal defense or land reclamation. By using our results, it is possible to determine at what stage a marsh restoration is by looking at sediment fluxes and UVVR, what would be the final outcome of the restoration, and the equilibrium timescale.

6. Open Research

Data points of Fig. 3 and Fig. 4 as well as an example of simulation output files are available at https://doi.org/10.5281/zenodo.5207786. A copy of the model codes was uploaded to and downloadable at https://zenodo.org/record/6028165#.YgwXivXMI60. This study was supported by the Department of the Interior Hurricane Sandy Recovery program (ID G16AC00455), NSF awards 1637630 (PIE LTER) and 1832221 (VCR LTER), and CSC (China Scholarship Council). Any use of trade, firm, or product names is for descriptive purposes only and does not imply endorsement by the U.S. Government.

References:

Ai, W., Li, M. T., Liu, X. Q., Li, W. H., Niu, S. J., & Tong, M. (2018). Hydrodynamics of ssc peak in dry season of the south passage of changjiang river estuary. *Oceanologia et Limnologia Sinica*, *49*(4). https://doi.org/10.11693/hyhz20171000273

Alizad, K., Hagen, S. C., Morris, J. T., Bacopoulos, P., Bilskie, M. v., Weishampel, J. F., & Medeiros, S. C. (2016). A coupled, two-dimensional hydrodynamic-marsh model with biological feedback. *Ecological Modelling*, *327*, 29–43. https://doi.org/10.1016/j.ecolmodel.2016.01.013

Barbier, E. B., Koch, E. W., Silliman, B. R., Hacker, S. D., Wolanski, E., Primavera, J., Granek, E. F., Polasky, S., Aswani, S., Cramer, L. A., Stoms, D. M., Kennedy, C. J., Bael, D., Kappel, C. v., Perillo, G. M. E., & Reed, D. J. (2008). Coastal ecosystem-based management with nonlinear ecological functions and values. *Science*, *319*(5861). https://doi.org/10.1126/science.1150349

Bayraktarov, E., Saunders, M. I., Abdullah, S., Mills, M., Beher, J., Possingham, H. P., Mumby, P. J., & Lovelock, C. E. (2016). The cost and feasibility of marine coastal restoration. *Ecological Applications*, *26*(4). https://doi.org/10.1890/15-1077

Beudin, A., Kalra, T. S., Ganju, N. K., & Warner, J. C. (2017). Development of a coupled wave-flow-vegetation interaction model. *Computers and Geosciences*, *100*, 76–86. https://doi.org/10.1016/j.cageo.2016.12.010

Brown, J. M., & Davies, A. G. (2010). Flood/ebb tidal asymmetry in a shallow sandy estuary and the impact on net sand transport. *Geomorphology*, *114*(3). https://doi.org/10.1016/j.geomorph.2009.08.006

Cole, S. W. (1994). Marsh Formation in the Borsippa Region and the Course of the Lower Euphrates. *Journal of Near Eastern Studies*, *53*(2). https://doi.org/10.1086/373672

Costanza, R., Pérez-Maqueo, O., Martinez, M. L., Sutton, P., Anderson, S. J., & Mulder, K. (2008). The value of coastal wetlands for hurricane protection. *Ambio*, *37*(4). https://doi.org/10.1579/0044-7447(2008)37[241:TVOCWF]2.0.CO;2

Crooks, S., Herr, D., Tamelander, J., Laffoley, D., & Vandever, J. (2011). Mitigating Climate Change through Restoration and Management of Coastal Wetlands and Near-shore Marine Ecosystems: Challenges and Opportunities. *Environment Department Papers*, *121*(121).

D'Alpaos, A., Lanzoni, S., Marani, M., & Rinaldo, A. (2007). Landscape evolution in tidal embayments: Modeling the interplay of erosion, sedimentation, and vegetation dynamics. *Journal of Geophysical Research: Earth Surface*, *112*(1). https://doi.org/10.1029/2006JF000537

DeLaune, R. D., Patrick, W. H., & Breemen, N. van. (1990). Processes governing marsh formation in a rapidly subsiding coastal environment. *Catena*, *17*(3). https://doi.org/10.1016/0341-8162(90)90021-5

Duarte, C. M., Dennison, W. C., Orth, R. J. W., & Carruthers, T. J. B. (2008). The charisma of coastal ecosystems: Addressing the imbalance. In *Estuaries and Coasts* (Vol. 31, Issue 2). https://doi.org/10.1007/s12237-008-9038-7

Elias, E. P. L., van der Spek, A. J. F., Wang, Z. B., & de Ronde, J. (2012). Morphodynamic development and sediment budget of the Dutch Wadden Sea over the last century. *Geologie En Mijnbouw/Netherlands Journal of Geosciences*, *91*(3). https://doi.org/10.1017/S0016774600000457

Fagherazzi, S., & Priestas, A. M. (2010). Sediments and water fluxes in a muddy coastline: Interplay between waves and tidal channel hydrodynamics. *Earth Surface Processes and*

Landforms, *35*(3). https://doi.org/10.1002/esp.1909

Fagherazzi, S., Kirwan, M. L., Mudd, S. M., Guntenspergen, G. R., Temmerman, S., D'Alpaos, A., van de Koppel, J., Rybczyk, J. M., Reyes, E., Craft, C., & Clough, J. (2012). Numerical models of salt marsh evolution: Ecological, geomorphic, and climatic factors. *Reviews of Geophysics*, *50*(1). https://doi.org/10.1029/2011RG000359

Fagherazzi, S., Mariotti, G., & Wiberg, P. L. (2013). Marsh collapse does not require sea level rise. *Oceanography*, *26*(3). https://doi.org/10.5670/oceanog.2013.47

Fleri, J. R., Lera, S., Gerevini, A., Staver, L., & Nardin, W. (2019). Empirical observations and numerical modelling of tides, channel morphology, and vegetative effects on accretion in a restored tidal marsh. *Earth Surface Processes and Landforms*, *44*(11), 2223–2235. https://doi.org/10.1002/esp.4646

Ganju, N. K. (2019). Marshes Are the New Beaches: Integrating Sediment Transport into Restoration Planning. *Estuaries and Coasts*, *42*(4). https://doi.org/10.1007/s12237-019-00531-3

Ganju, N. K., Defne, Z., Kirwan, M. L., Fagherazzi, S., D'Alpaos, A., & Carniello, L. (2017). Spatially integrative metrics reveal hidden vulnerability of microtidal salt marshes. *Nature Communications*, *8*. https://doi.org/10.1038/ncomms14156

Kalra, T. S., Ganju, N. K., Aretxabaleta, A. L., Carr, J. A., Defne, Z., & Moriarty, J. M. (2021). Modeling Marsh Dynamics Using a 3-D Coupled Wave-Flow-Sediment Model. *Frontiers in Marine Science*, *8*. https://doi.org/10.3389/fmars.2021.740921

Kirwan, M. L., & Murray, A. B. (n.d.). *A coupled geomorphic and ecological model of tidal marsh evolution* (Vol. 104, Issue 15).

Mariotti, G., & Canestrelli, A. (2017). Long-term morphodynamics of muddy backbarrier basins: Fill in or empty out? *Water Resources Research*, *53*(8), 7029–7054. https://doi.org/10.1002/2017WR020461

Mariotti, G., & Fagherazzi, S. (2010). A numerical model for the coupled long-term evolution of salt marshes and tidal flats. *Journal of Geophysical Research: Earth Surface*, *115*(1). https://doi.org/10.1029/2009JF001326

Marjoribanks, T. I., Hardy, R. J., & Lane, S. N. (2014). The hydraulic description of vegetated river channels: the weaknesses of existing formulations and emerging alternatives. *Wiley Interdisciplinary Reviews: Water*, *1*(6). https://doi.org/10.1002/wat2.1044

Mckee, K. L., & Patrick, W. H. (1988). The Relationship of Smooth Cordgrass (Spartina alterniflora) to Tidal Datums: A Review. In *Source: Estuaries* (Vol. 11, Issue 3). https://www.jstor.org/stable/1351966?seq=1&cid=pdf-

Mcowen, C. J., Weatherdon, L. v., van Bochove, J. W., Sullivan, E., Blyth, S., Zockler, C., Stanwell-Smith, D., Kingston, N., Martin, C. S., Spalding, M., & Fletcher, S. (2017). A global map of saltmarshes. *Biodiversity Data Journal*, *5*(1). https://doi.org/10.3897/BDJ.5.e11764

Möller, I., Kudella, M., Rupprecht, F., Spencer, T., Paul, M., van Wesenbeeck, B. K., Wolters, G., Jensen, K., Bouma, T. J., Miranda-Lange, M., & Schimmels, S. (2014). Wave attenuation over coastal salt marshes under storm surge conditions. *Nature Geoscience*, *7*(10). https://doi.org/10.1038/NGEO2251

Morris, J. T. (2006). Competition among marsh macrophytes by means of geomorphological displacement in the intertidal zone. *Estuarine, Coastal and Shelf Science*, *69*(3–4). https://doi.org/10.1016/j.ecss.2006.05.025

Morris, J. T., & Haskin, B. (1990). A 5-yr record of aerial primary production and stand characteristics of Spartina alterniflora. *Ecology*, *71*(6). https://doi.org/10.2307/1938633

Mudd, S. M., Fagherazzi, S., Morris, J. T., & Furbish, D. J. (2004). *9 Flow, Sedimentation, and Biomass Production on a Vegetated Salt Marsh in South Carolina: Toward a Predictive Model of Marsh Morphologic and Ecologic Evolution*. https://doi.org/10.1029/##CE

Narayan, S., Beck, M. W., Wilson, P., Thomas, C. J., Guerrero, A., Shepard, C. C., Reguero, B. G., Franco, G., Ingram, J. C., & Trespalacios, D. (2017). The Value of Coastal Wetlands for Flood Damage Reduction in the Northeastern USA. *Scientific Reports*, *7*(1). https://doi.org/10.1038/s41598-017-09269-z

Nardin, W., & Edmonds, D. A. (2014). Optimum vegetation height and density for inorganic sedimentation in deltaic marshes. *Nature Geoscience*, *7*(10). https://doi.org/10.1038/NGEO2233

Nardin, W., Edmonds, D. A., & Fagherazzi, S. (2016). Influence of vegetation on spatial patterns of sediment deposition in deltaic islands during flood. *Advances in Water Resources*, *93*. https://doi.org/10.1016/j.advwatres.2016.01.001

Pingree, R. D., & Griffiths, D. K. (1979). Sand transport paths around the british isles resulting from m2 and m4 tidal interactions. *Journal of the Marine Biological Association of the United Kingdom*, *59*(2). https://doi.org/10.1017/S0025315400042806

Secretariat of the Convention on Biological Diversity. (2007). *Biodiversity*, *8*(4). https://doi.org/10.1080/14888386.2007.9712830

Seddon, N., Daniels, E., Davis, R., Chausson, A., Harris, R., Hou-Jones, X., Huq, S., Kapos, V., Mace, G. M., Rizvi, A. R., Reid, H., Roe, D., Turner, B., & Wicander, S. (2020). Global recognition of the importance of nature-based solutions to the impacts of climate change. *Global Sustainability*, *3*. https://doi.org/10.1017/sus.2020.8

Sheng, Y. P., Lapetina, A., & Ma, G. (2012). The reduction of storm surge by vegetation canopies: Three-dimensional simulations. *Geophysical Research Letters*, *39*(20). https://doi.org/10.1029/2012GL053577

Staver, L. W., Stevenson, J. C., Cornwell, J. C., Nidzieko, N. J., Staver, K. W., Owens, M. S., Logan, L., Kim, C., & Malkin, S. Y. (2020). Tidal Marsh Restoration at Poplar Island: II. Elevation Trends, Vegetation Development, and Carbon Dynamics. *Wetlands*. https://doi.org/10.1007/s13157-020-01295-4

Temmerman, S., Bouma, T. J., Govers, G., Wang, Z. B., de Vries, M. B., & Herman, P. M. J. (2005). Impact of vegetation on flow routing and sedimentation patterns: Three-dimensional modeling for a tidal marsh. *Journal of Geophysical Research: Earth Surface*, *110*(4). https://doi.org/10.1029/2005JF000301

Temmerman, S., Meire, P., Bouma, T. J., Herman, P. M. J., Ysebaert, T., & de Vriend, H. J. (2013). Ecosystem-based coastal defence in the face of global change. In *Nature* (Vol. 504, Issue 7478). https://doi.org/10.1038/nature12859

VanZomeren, C. M., Berkowitz, J. F., Piercy, C. D., & White, J. R. (2018). Restoring a degraded marsh using thin layer sediment placement: Short term effects on soil physical and biogeochemical properties. *Ecological Engineering*, *120*. https://doi.org/10.1016/j.ecoleng.2018.05.012

Vona, I., Gray, M. W., & Nardin, W. (2020). The impact of submerged breakwaters on sediment distribution along marsh boundaries. *Water (Switzerland)*, *12*(4). https://doi.org/10.3390/W12041016

Warner, J. C., Armstrong, B., He, R., & Zambon, J. B. (2010). Development of a Coupled Ocean-Atmosphere-Wave-Sediment Transport (COAWST) Modeling System. *Ocean Modelling*, *35*(3). https://doi.org/10.1016/j.ocemod.2010.07.010

Wigand, C., Ardito, T., Chaffee, C., Ferguson, W., Paton, S., Raposa, K., Vandemoer, C., & Watson, E. (2017). A Climate Change Adaptation Strategy for Management of Coastal Marsh Systems. *Estuaries and Coasts*, *40*(3). https://doi.org/10.1007/s12237-015-0003-y

Zedler, J. B., & Kercher, S. (2005). Wetland resources: Status, trends, ecosystem services, and restorability. In *Annual Review of Environment and Resources* (Vol. 30). https://doi.org/10.1146/annurev.energy.30.050504.144248

Zhao, H., & Chen, Q. (2014). Modeling Attenuation of Storm Surge over Deformable Vegetation: Methodology and Verification. *Journal of Engineering Mechanics*, *140*(12). https://doi.org/10.1061/(asce)em.1943-7889.0000704